WFL Publisher
Science and Technology
Meri-Rastilantie 3 B, FI-00980
Helsinki, Finland
e-mail: info@world-food.net

Journal of Food, Agriculture & Environment Vol.10 (2): 803-809. 2012

www.world-food.net

A multi-temporal Landsat TM data analysis of the impact of land use and land cover changes on the urban heat island effect

Qijiao Xie [1, 2], Zhixiang Zhou [1]*, Mingjun Teng [1] and Pengcheng Wang [1]

[1]College of Horticultural & Forestry Science/Key Laboratory of Horticultural Plant Biology (Ministry of Education), Huazhong Agricultural University, Wuhan 430070, China. [2]School of Resources and Environmental Science, Hubei University, Wuhan, 430062, China. e-mail: whzhouzx@mail.hzau.edu.cn, xieqijiao@126.com, tonny_cn@msn.com, pengchengwang@163.com

Received 30 January 2012, accepted 2 May 2012.

Abstract

The drastic change in land use/land cover (LULC) associated with urbanization is a powerful driving force in local climate and environment changes. The urban heat island (UHI) effect, a phenomenon that air and surface temperatures are higher in urban areas than in rural areas, is closely related to changes in LULC. In this study, remote sensing techniques were applied to derive information on LULC and land surface temperature (LST). The multi-temporal Landsat-5 Thematic Mapper (TM) images of 1987, 1996 and 2007 were used to detect the LULC changes and analyze their impacts on LST distributions and the UHI patterns. Results revealed that Wuhan has experienced an ongoing and accelerated urbanization from 1987 to 2007 with the urban built-up area increasing by nearly 303.14%. However, the UHI intensity was found to not always present a linear trend with the expansion of built-up area. It was partly influenced by the seasonal land cover variation associated with agricultural activities. For each land cover, the mean LST and area proportion of different LST classes were counted. Results indicated that water and forest had relatively lower surface temperatures and built-up and bare land areas had higher ones. Only 0.01% to 1.60% of the water areas were identified as heat islands, while sub-high and high temperatures were recorded in more than 90% of the built-up areas and nearly 80% of the bare land areas. These findings can provide useful information for urban planning, greening design and environmental management.

Key words: LST, UHI, NDVI, urbanization, remote sensing, land use/land cover, TM imagery.

Introduction

Rapid urbanization results in a tremendous growth of population and buildings in cities, as well as an increasing replacement of natural landscapes by impervious surface areas. With the reduction in vegetated area and an increase in impervious area, land surface soil water content and vegetation cover are modified[1]. These modifications consequently alter the surface radiative, thermal and moisture properties over urban areas [2], which then influence the thermal balance by altering the sensible and latent heat exchange between the urban surface and boundary layers [3]. Urban areas typically have higher solar radiation absorption and a greater thermal capacity and conductivity and consequently experience higher surface and air temperatures when compared to the surrounding rural areas, known as urban heat island (UHI) effect [4]. Increased temperatures may increase the air conditioning demands and energy use in urban areas, which in turn warms up the urban environment [5]. The sustaining higher temperatures alter the local climate, raise air pollution level and then lead to thermal discomfort and incidences of heat-related illness in urban areas [6].

Traditionally, UHI detection has been conducted in isolated locations with the air temperature data from *in situ* measurements, weather stations or automobile transects [4]. These fieldwork study methods provide accurate and real air temperatures at small scales. However, collecting measurements is time consuming and easily influenced by the immediate environment, which limits the application on a larger scale. Satellite remote sensing technology has made it possible to study UHI effect both remotely and regionally [7]. Remotely sensed image data, including NOAA AVHRR [7-9], MODIS [10], airborne ATLAS [11] and Landsat TM/ETM+ [12-14], have been used to derive land surface temperature (LST) and examine the UHI effect on vast territories. Results show that satellite-retrieved LST data have relatively higher spatial resolutions and are less time-consuming compared to ground measurement data. The application of coarse spatial resolution remotely sensed data in examining the UHI is requisite and informative in metropolitan areas. The studies on LST indicated that LST values varied with surface cover characteristics, such as soil water content and vegetation cover. This finding encourages more and more research focusing on the relationship between LST and the normalized difference vegetation index (NDVI) or other vegetation-related indices in previous studies [1, 11-12, 15-18].

The drastic change in land use/land cover (LULC) associated with human activities is regarded as a powerful driving force in local climate and environment changes [19, 20]. UHI intensity is closely related to LULC patterns over time. Therefore, accurate detection on LULC changes associated with urbanization and LST distribution is critical to environmental monitoring, management and planning [21]. For this research, much emphasis was placed on determining the urban LULC changes and their impact on LST patterns and UHI distribution at the local and regional level [13, 18, 22-25]. Results show that the proportion of non-vegetated and impervious areas dramatically increased in almost all the studied cities as these have experienced rapid urbanization in recent years.

The tremendous LULC changes in urban and developed rural areas exacerbated the UHI effect at a regional scale. The bare soil, waste land and urban developed areas (industrial area, commercial area and high dense residential area) were observed to have relatively higher surface temperatures, compared to water bodies, green spaces and agricultural land.

The objective of this study was to detect LULC changes and their impact on LST distribution and UHI extent from 1987 to 1996 then to 2007 in a rapidly urbanizing area of central China, using multi-temporal Landsat TM images. The hybrids classification method was used to classify the image pixels into six land covers: farmland, forest, grassland, built-up area, water and bare land. The LST values were derived from the Landsat TM thermal infrared band (band 6) after radiometric and atmospheric corrections were made. The thermal response and the UHI extent in different land covers were analyzed over three years.

Materials and Methods

Study area and data: Wuhan is the capital of Hubei province, situated at 113°41'~115°05'E, 29°58'~31°22'N. It is located in the east of the Jianghan Plain and at the confluence of the middle reaches of the Yangtze River and Han River. The rivers divide the metropolitan area into three parts, namely Wuchang, Hankou and Hanyang. The city covers an area of 8,467 km^2 with a built-up area of 460.8 km^2 and a population of about 8.31 million. It is recognized as the political, economic, educational and transportation center of central China. Mean annual temperature ranges from 15.8 to 17.5ºC and annual frost free period lasts 211 to 272 days. The mean annual precipitation is 1269 mm, with 40% occurring during June to August.

Wuhan has experienced rapid urbanization over the last three decades since China's 'Open and Reform Policy' started at the end of the 1970s, a process which accelerated in the recent two decades. The digital remote sensing method provides an overall investigation on the urbanization and associated climate change at a city scale. In this study, three Landsat-5 TM images acquired on September 26, 1987, October 4, 1996 and April 10, 2007 were selected. The Landsat images were rectified to the Universal Transverse Mercator (UTM) projection system (spheroid WGS84, datum WGS84, zone 50) and were georeferenced to a digital road map of 2008 with a scale of 1:100,000 for Wuhan city.

Land cover classification: Urban LULC pattern is important in indicating the conditions and functions of urban ecosystem [26]. Land cover modifications due to urban development affect the urban energy balance and thermal environment by altering covering materials and consequent surface characteristics and properties. Multi-temporal images in monitoring LULC changes are very useful in identifying the environmental variation (e.g. UHI effect) over time. Unsupervised classification was initially performed for the three satellite images and produced 12 classes due to the overall spectral separability. Supervised classication was then undertaken using Maximum likelihood classification [24,25,27]. The overall accuracies of classification and kappa coefficients for 1987, 1996 and 2007 were 87.54%, 92.39% and 89.13% and 0.83, 0.90 and 0.86, respectively.

In this study, all of the pixels for each digital satellite image were grouped into six types, including:

(1) Farmland: defined as arable or cultivable land including both cropped and temporarily fallow land. Cropped land refers to land under annual crops, such as cereals, cotton, wheat and vegetables. Orchards with permanent crops (e.g. fruit plantations) were excluded from this class.

(2) Forest: includes any type of vegetation that can provide canopy cover and shadow, typically referring to all of the deciduous and evergreen trees and shrubs.

(3) Grassland: includes residential lawns, parks, and golf courses and does not include areas covered by annual crops.

(4) Built-up: refers to the impervious surface in urban areas including buildings, parking lots and roadways.

(5) Water: refers to all of the water bodies in the study area, including the Yangtze River, the Han River, lakes, wetlands, fish ponds and other rivers.

(6) Bare land: refers to the unused and barren soil.

Derivation of LST from TM imageries: When using multi-temporal satellite images in quantitative retrieval of NDVI and LST, it is crucial to eliminate the atmospheric effect by radiometric correction and atmospheric correction. The original digital number (DN) from TM images was converted into at-sensor radiance by using gain and offset values which can be obtained from the header file of the images [28, 29]. Top of the atmosphere (TOA) reectance was then calculated based on the radiance value according to Chander *et al.* [29]:

$$\rho = \frac{\pi L d^2}{E_0 \cos\theta} \tag{1}$$

where ρ is the TOA reectance, L is the at-sensor radiance for a given band, d is the Earth–Sun distance in astronomical unit, usually about 1, E_0 is mean solar exoatmospheric spectral irradiances and θ is Zenithal Solar Angle. Usage of the TOA reectance in multi-temporal satellite images eliminates the effect of solar zenith angles and Earth–Sun distances on the quantitative output. For this study, the corrections of TM images were necessary for derivation of LST and NDVI but unnecessary for LULC classification.

The NDVI was usually used to express the vegetation amount and fractional vegetation cover when studying the urban climate. It is very sensitive to the absorption and reection of the Landsat TM red (band 3) and infrared bands (band 4). Therefore, NDVI can be calculated from these two bands through the formula:

$$NDVI = (\rho(band\,4)) - (\rho(band\,3)) / (\rho(band\,4)) + (\rho(band\,3)) \tag{2}$$

where ρ (*band* 4) and ρ (*band* 3) are TOA reectances for band 4 and band 3, respectively, which can be obtained from Eq. 1 above. LST plays an important role in exchanging energy, water and heat flux between land surface and atmosphere. Satellite remote sensing provides an informative method to examine LST distribution and UHI pattern at local and regional scale. The derivation of LST from Landsat TM thermal infrared (*band 6*) was employed in Erdas imagine 9.2 following several steps: radiometric calibration, brightness temperature calculation, atmospheric and surface emissivity corrections and LST estimation. Firstly, the DN values from band 6 of TM image were converted to spectral radiances according to previous literatures:

$$L_{sat} = G_{ain} \times DN + Off_{set}$$ [28, 29].

The next step was to convert the spectral radiance into a satellite brightness temperature (T_{sensor}) with the equation [28]:

$$T_{\text{sensor}} = \frac{K_2}{\ln(1 + K_1 / L_{sat})} \quad (3)$$

The T_{sensor} values obtained are referenced to a black body, regarding the emissivity is uniform. Therefore, it is necessary to correct the spectral emissivity (ε) according to the nature of land cover [12]. Urban impervious areas and bare soil were assigned a value of 0,923 and water 0.9925 [30-31]. For natural land cover, there was a modeling relationship with NDVI values through field measurement:

$$\varepsilon = 1.0094 + 0.047 Ln(NDVI)$$ [32].

Based on satellite brightness temperature (T_{sensor}) and the corrected emissivity (ε), LST values can be computed through the following equation [33]:

$$LST = \frac{T_{sensor}}{1 + (\lambda \times T_{sensor} / \rho) \ln \varepsilon} \quad (4)$$

The constants used in Eq. 3 and Eq. 4 were obtained from the previous literatures [28, 33].

Urban heat island identification: Considering the seasonable differences in temperature range and atmospheric conditions among multi-temporal TM images, we used the UHI intensity rather than the temperature values in the landcover-related analysis. The LST values were divided into five classes (low, sub-low, medium, sub-high and high temperature) based on the mean and standard deviation (SD) of the temperature distribution [34].

$$T = T_0 \pm X * SD \quad (5)$$

where T is the threshold value, T_0 is the mean temperature of the study area, SD is the standard deviation of LST, and X is assigned values of 0.5 and 1.5.

Results and Discussion

LULC changes from 1987 to 2007: Fig. 1 illustrates the LULC distribution maps derived from the three TM images. Although there were significant differences in built-up extent between the LULC maps, they shared similar spatial LULC patterns. The built-up area was mainly located at the city core and embraced by a large area of farmland. Together with the other water bodies, the Yangtze River and Han River accounted for a large percentage of the study area. They formed the main "blue corridors" running through the city. The main concentration of forests was distributed in the north and northeast of the study area. Table 1 indicates the detailed statistical area of different LULC types for 1987, 1996 and 2007. From this table, similar patterns in area proportion for LULC types were found. The largest area was farmland, followed by water, forest, built-up area, grassland and bare land.

Table 2 represents the area changes of different types of land cover from 1987 to 2007. The largest areal change appeared in

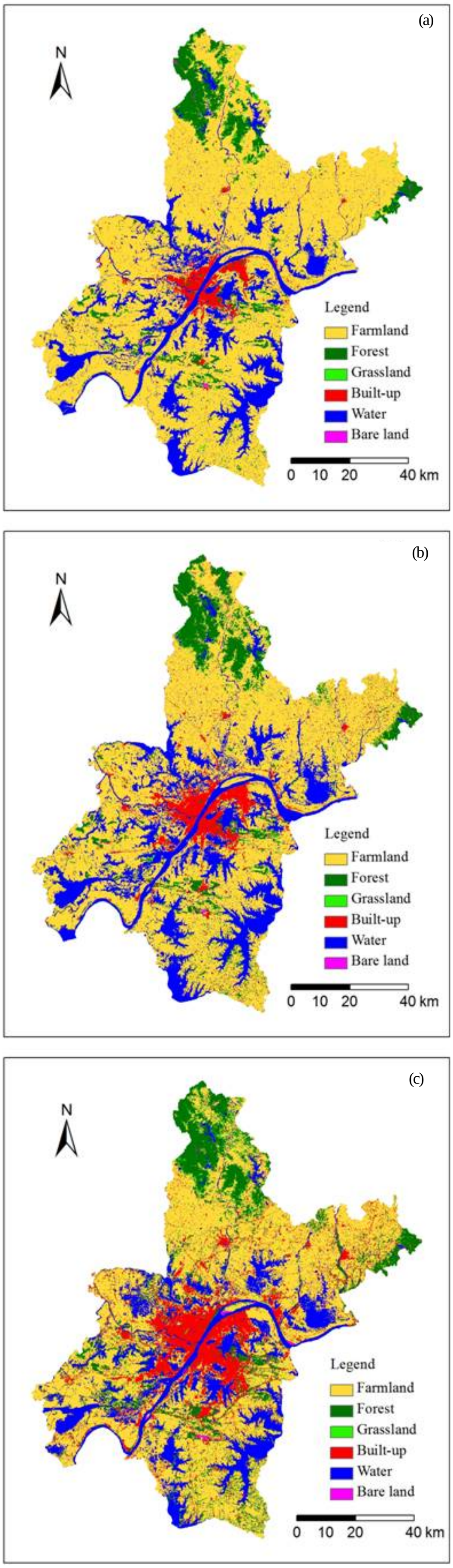

Figure 1. The LULC distribution maps in 1987 (a), 1996 (b) and 2007 (c).

Table 1. Area statistics (km^2) for different LULC types in 1987, 1996 and 2007.

LULC type	1987		1996		2007	
	Area	%	Area	%	Area	%
Farmland	5872.95	68.43	5181.57	60.37	4511.51	52.60
Forest	724.36	8.44	825.70	9.62	1197.51	13.96
Grassland	56.06	0.65	81.18	0.95	123.07	1.43
Built-up	287.36	3.35	522.93	6.09	1158.47	13.51
Water	1631.94	19.01	1948.71	22.71	1560.02	18.19
Bare land	10.16	0.12	22.48	0.26	26.91	0.31

Table 2. Area changes (km^2) of each LULC type among the three observed years.

LULC type	1987-2007		1987-1996		1996-2007	
	Area change	%	Area change	%	Area change	%
Farmland	-1361.44	-23.18	-691.38	-11.77	-670.06	-12.93
Forest	473.15	65.32	101.34	13.99	371.81	45.03
Grassland	67.01	119.53	25.12	44.81	41.89	51.60
Built-up	871.11	303.14	235.57	81.98	635.54	121.53
Water	-71.92	-4.41	316.77	19.41	-388.69	-19.95
Bare land	16.75	164.86	12.32	121.26	4.43	19.71

built-up cover with an increase of 871.11 km^2 (303.14%) from 287.36 km^2 in 1987 to 1158.47 km^2 in 2007. This wider variation in urbanized area illustrates that the city experienced rapid urbanization during those two decades. Meanwhile, the areas of bare land and grassland were found to have obvious increases of about 164.86% and 119.53%. Following this was forest type, which increased by nearly 65.32%. However, farmland areas decreased by about 23.18% from 5872.95 km^2 in 1987 to 4511.51 km^2 in 2007. Water areas decreased moderately, by about 3.41%. The area changes in farmland, forest and grassland in this 20-year period were partly due to the Project of Conversion of Farmland to Forest and Grassland [35]. This project was carried out to stop deforestation for farmland reclamation, protect natural forests and reforest the formerly cultivated land, which efficiently increased forest and grassland areas and consequently decreased farmland areas.

Table 2 also illustrates varying speeds of change for different LULC types from 1987 to 1996 and then to 2007. The largest difference was found in built-up area. The areas increased by 81.98% from 1987 to 1996 and 121.53% from 1996 to 2007, which means that the built-up areas increased by nearly 9.11% and 11.05% each year, respectively. The most complex change occurred in the water type with an increase of 19.41% from 1987 to 1996 and a decrease of 19.95% from 1996 to 2007. This is because the seasonal variation in precipitation influences the classification of water type. The mean precipitation from June to September was 567.8 mm in 1987 and 767.9 mm in 1996 (Hubei Statistical Yearbook), which could explain, to some extent, the increase in water area from 1987 to 1996, but perhaps most importantly, the TM image used for LULC classification in 2007 was acquired on April, 10, when rainfall is rare. Some fish ponds and small water bodies were dry at this time, and so these areas were classified into other land cover types. This can explain the water area decrease from 1996 to 2007.

Thermal response of LULC: Understanding the thermal response of individual land covers within a city is valuable to observe the impact of LULC change on the LST. The mean LST values for each type of LULC in 1987, 1996 and 2007 are summarized in Table 3. Generally, water type exhibits the lowest mean temperatures as compared to other land cover types. The built-up area and bare land were found to have similarly higher temperatures due to the high heat capacity and thermal conductivity of the surface materials. The detailed information on the LST difference between different land cover types shows an increasing gradation in thermal response from water to farmland to forest to grassland to bare land and finally to built-up areas in both 1987 and 1996, while a warming trend from water to forest to farmland to grassland to built-up area then to bare land in 2007. The farmland cover was found to be similar in thermal response to the forest cover in 1987 and 1996, while it was similar to grassland in 2007. This is because the farmland was fully covered by crops in 1987 and 1996 with larger amount of biomass and higher vegetation cover, while it was partly unoccupied in 2007 (late spring).

Impact of LULC changes on UHI: The significant difference in mean LST values between different land covers mentioned above (Table 3) indicated that an obvious UHI effect existed in the study area. Fig. 2 shows the UHI distribution maps, which were produced by assigning the LST threshold values based on the mean temperatures and the SDs of LST (Table 4). The surface temperatures were divided into five classes (low, sub-low, medium, sub-high and high temperatures), among which the class of high temperature was identified as the intensive heat island. It is evident from the maps that some hot spots, warm corridors and heat islands can be easily identified for the three observed years. The heat islands of 1987 and 1996 were mainly distributed in the center of

Table 3. Mean land surface temperatures (°C) for different LULC types.

LULC type	September 26.1987		October 4,1996		April 10, 2007	
	Mean LSTs	SD	Mean LSTs	SD	Mean LSTs	SD
Farmland	39.97	4.26	24.20	2.15	23.57	2.51
Forest	40.38	5.17	24.23	1.87	22.12	2.09
Grassland	44.01	5.44	25.78	2.81	24.07	1.77
Built-up	47.86	4.36	29.37	1.37	26.17	1.63
Water	32.80	10.41	21.20	0.85	16.32	2.16
Bare land	46.07	5.86	26.43	2.21	27.48	3.98

Table 4. Statistics of land surface temperatures (°C) for September 26, 1987, October 4, 1996 and April 10, 2007.

Year	Max	Min	Mean	SD
1987	62.8	29.7	39.6	4.69
1996	34.2	19.5	23.91	2.5
2007	35.72	12.35	22.41	3.84

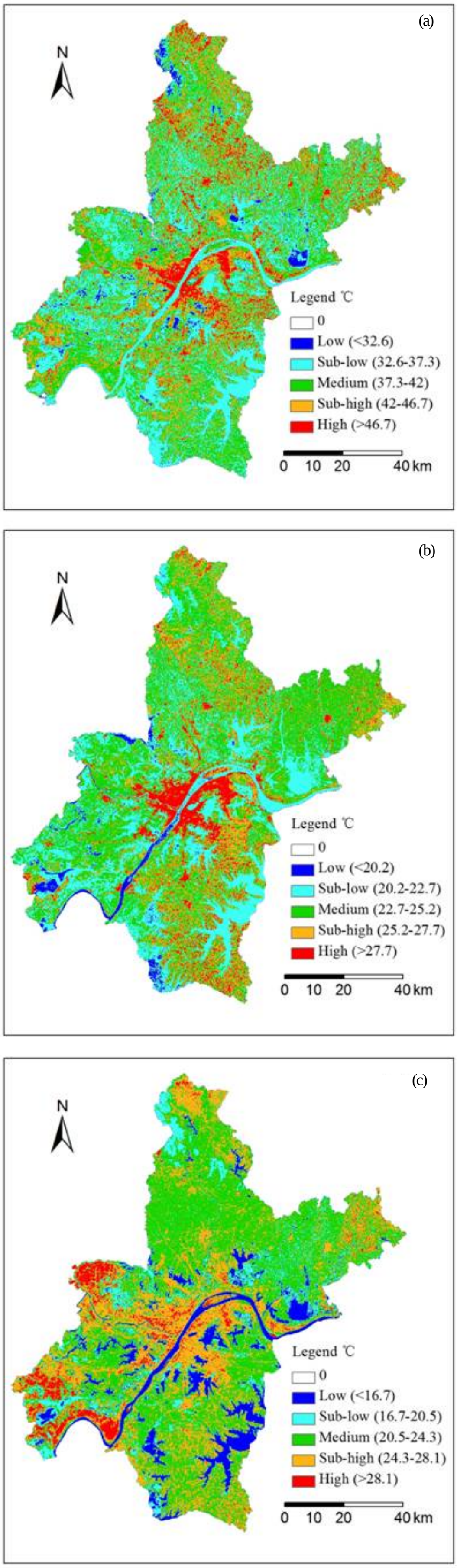

Figure 2. The UHI distribution maps for September 26,1987 (a), October 4,1996 (b) and April 10, 2007 (c).

the city, with the UHI extent obviously expanding from 1987 to 1996. However, the heat islands in 2007 spread from the urban core to the west corner of the city with a relatively weaker UHI intensity in built-up areas.

When masking the LULC maps over the corresponding UHI maps for the three studied years, a noticeable result appeared. The UHI did not always correspond to the urbanized area, though there was an ongoing expansion in built-up areas. Results indicated that the LULC change can better explain the associated UHI variation during 1987 to 1996 than 1996 to 2007, which could be interpreted in various ways. Firstly, Wuhan experienced a rapid urbanization during 1987 to 1996 without highly considering the urban environmental protection, while after 1996, a series of ecological restoration projects (e.g., Project of Conversion of Farmland to Forest and Grassland and Soil and Water Conservation) were carried out to improve urban air quality. These projects enhanced the vegetation cover and biomass amount in urban areas, which then consequently reduced the urban-rural temperature differences and mitigated the UHI effect during 1996 to 2007. Secondly, the seasonal variation of land surface temperatures could partly influence the relationship between LULC changes and UHI pattern, as expected. In addition, agricultural activities resulted in periodic variation in farmland cover, which could significantly impact the vegetation cover and biomass amount seasonally.

UHI effect and intensity varies with land cover type and associated properties. For each land cover, the area proportion of different LST classes was counted for the three observed years, as shown in Fig. 3. It indicates that only 0.01% to 1.60% of the water areas were identified as heat islands, with most areas classed into the classes of low and sub-low temperature. However, more than 90% built-up areas and nearly 80% of the bare land areas were occupied by sub-high and high temperatures, indicating UHI effect frequently occurred in these two land covers. This is because they are fully exposed to solar radiation without canopy shading and evaporative cooling effect. For the vegetated types of farmland, forest and grassland, the UHI area percentage varied with the vegetation area, canopy shading area and biomass amount within the given type. Generally, the UHI effect occurred more frequently in grassland than in forest. In other words, forest cover was found to be more effective at mitigating UHI effect than grassland due to the dense foliage and complex canopy structure.

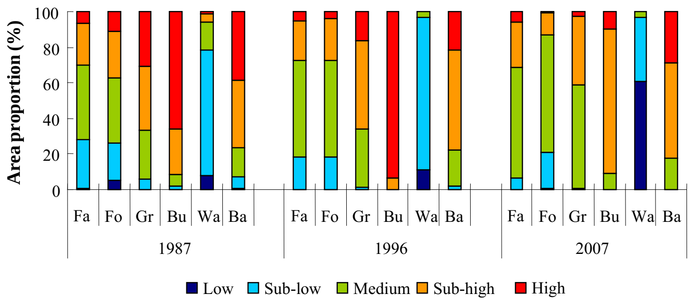

Figure 3. The area proportion of LST classes for each LULC type in the three studied years (Fa: farmland, Fo: forest, Gr: grassland, Bu: buit-up, Wa: water, Ba: bare land).

Conclusions

In this study, three multi-temporal TM images of 1987, 1996 and 2007 were used to detect the LULC changes and associated LST and UHI effect variations in Wuhan, China. The Landsat remote sensing method provides informative data in investigating the impact of LULC change on LST from 1987 to 2007 at a city scale. Results showed that during the period of 1987 to 2007, built-up areas increased by nearly 303.14%. Economic development in the study area accelerated the urbanization process, leading to a growth rate of built-up area of 9.11% during 1987 to 1996 and 11.05% during 1996 to 2007. Farmland area decreased by nearly 23.18% with the area increase of 65.32% in forest and 119.53% in grassland during the studied period partly due to the Project of Conversion of Farmland to Forest and Grassland.

The mean LST values of different land covers derived from TM images helps to better understand the thermal response of surface materials. Results showed that the water bodies and forests had relatively lower surface temperatures and were efficient in decreasing urban LST and mitigating the UHI effect. This encourages urban planners and greening designers to devote more efforts in protecting urban lakes and forests. On the other hand, built-up area and bare land were detected as the main heat islands in observed area, as expected. The thermal response of farmland was similar to the forest when the farmland was covered by growing and exuberant crops, while similar to the grassland when not occupied.

Landsat remote sensing images were ideal to analyze the LULC changes and UHI effect temporally and spatially at a city scale. However, it is difficult to select multi-temporal images with similar conditions of atmosphere, season and vegetation cover. The radiometric correction and atmospheric correction were necessary to eliminate the atmospheric effect. In this study, considering seasonal differences in temperature range, LST was classified based on the mean LST value and associated SD of LST to identify the UHI effect. The relationship between LULC change and UHI effect was examined. Results indicated except for the urbanization, other human activities (for example, agricultural activities) also had significant influences on UHI effect. Further emphasis needs to be placed on the impact of human activities on LULC changes and consequent environmental result.

Acknowledgements

This research was sponsored by the Fund for Science and Technology Program of Wuhan (200951999569) and the Fundamental Research Funds for the Central Universities (Program No.2011PY045). The authors would like to thank Elizabeth Lord and the other reviewers for reviewing and correcting the paper.

References

[1]Owen, T. W., Carlson, T. N. and Gillies, R. R. 1998. An assessment of satellite remotely-sensed land cover parameters in quantitatively describing the climatic effect of urbanization. Int. J. Remote Sens. **19**:1663-1681.

[2]Oke, T. R. 1987. Boundary Layer Climates. Routledge,New York, 435 p.

[3]Yang, L., Xian, G., Klaver, J. M. and Deal, B. 2003. Urban land-cover change detection through sub-pixel imperviousness mapping using remotely sensed data. Photogramm. Eng. Rem. S. **69**(9):1003-1010.

[4]Voogt, J. A. and Oke, T. R. 2003. Thermal remote sensing of urban areas. Remote Sens. Environ. **86**:370-384.

[5]White, M. A., Nemani, R. R., Thornton, P. E. and Running, S. W. 2002. Satellite evidence of phenological differences between urbanized and rural areas of the eastern United States deciduous broadleaf forest. Ecosystems **5**:260–277.

[6]Poumadere, M., Mays, C., LeMer, S. and Blong, R. 2005. The 2003 heatwave in France: Dangerous climate change here and now. Risk Annual **25**(6):1483-1494.

[7]Streutker, D. R. 2003. Satellite-measured growth of the urban heat island of Houston, Texas. Remote Sens. Environ. **85**:282-289.

[8]Balling, R. C. and Brazell, S. W. 1988. High resolution surface temperature patterns in a complex urban terrain. Photogramm. Eng. Rem. S. **54**:1289-1293.

[9]Gallo, K. P. and Owen, T. W. 1998. Assessment of urban heat island: A multi-sensor perspective for the Dallas-Ft. Worth, USA region. Geocarto International **13**:35-41.

[10]Pu, R., Gong, P., Michishita, R. and Sasagawa, T. 2006. Assessment of multi-resolution and multi-sensor data for urban surface temperature retrieval. Remote Sens. Environ. **104**:211-225.

[11]Lo, C. P., Quattrochi, D. A. and Luvall, J. C. 1997. Application of high-resolution thermal infrared remote sensing and GIS to assess the urban heat island effect. Int. J. Remote Sens. **18**:287-304.

[12]Weng, Q., Lu, D. S. and Schubring, J. 2004. Estimation of land surface temperature-vegetation abundance relationship for urban heat island studies. Remote Sens. Environ. **89**:467-483.

[13]Chen, X. L., Zhao, H. M., Li, P. X. and Yin, Z. Y. 2006. Remote sensing image-based analysis of the relationship between urban heat island and land use/cover changes. Remote Sens. Environ. **104**:133-146.

[14]Zhang, Y. S., Odeh, Inakwu, O. A. and Han, C. F. 2009. Bi-temporal characterization of land surface temperature in relation to impervious surface area, NDVI and NDBI, using a sub-pixel image analysis. Int. J. Appl. Earth Obs. **11**(4):256-264.

[15]Price, J. C. 1990. Using spatial context in satellite data to infer regional scale evapotranspiration. IEEE T. Geosci. Remote. **28**:940–948.

[16]Gillies, R. R. and Carlson, T. N. 1995. Thermal remote sensing of surface soil water content with partial vegetation cover for incorporation into climate models. J. Appl. Meteorol. **34**:745-756.

[17]Raynolds, M. K., Comiso, J. C., Walker, D. A. and Verbyla, D. 2008. Relationship between satellite-derived land surface temperatures, arctic vegetation types, and NDVI. Remote Sens. Environ. **112**:1884-1894.

[18]Nonomura, A., Kitahara, M. and Masuda, T. 2009. Impact of land use and land cover changes on the ambient temperature in a middle scale city, Takamatsu, in Southwest Japan. J. Environ. Manage. **90**:3297-3304.

[19]Du, Y., Xie, Z. Q., Zeng, Y., Shi, Y. F. and Wu, J. G. 2007. Impact of urban expansion on regional temperature change in the Yangtze River Delta. J. Geogr. Sci. **17**:387-398.

[20]Shi, Z. H., Chen, L. D., Hao, J. P., Wang, T. W. and Cai, C. F. 2009. The effects of land use change on environmental quality in the red soil hilly region, China: A case study in Xianning County. Environ. Monit. Assess. **150**:295-306.

[21]Assefa, M. M. 2004. Spatiotemporal dynamics of land surface parameters in the Red River of the North Basin. Phys. Chem. Earth **29**:795-810.

[22]Li, J. J., Wang, X. R., Wang, X. J., Ma, W. C. and Zhang, H. 2009. Remote sensing evaluation of urban heat island and its spatial pattern of the Shanghai metropolitan area, China. Ecol. Complex. **6**:413-420.

[23]Hart, M. A. and Sailor, D. J. 2009. Quantifying the influence of land-use and surface characteristics on spatial variability in the urban heat island. Theor. Appl. Climatol. **95**:397-406.

[24]Kant, Y., Bharath, B. D., Mallick, J., Atzberger, C. and Kerle N. 2009. Satellite-based analysis of the role of land use/land cover and vegetation density on surface temperature regime of Delhi, India. J. Indian Soc. Remote Sens. **37**:201-214.

[25]Tan, K. C., Lim, H. S., MatJafri, M. Z. and Abdullah, H. 2010. Landsat data to evaluate urban expansion and determine land use/land cover changes in Penang Island, Malaysia. Environ. Earth Sci. **60**:1509-1521.

[26]Lunetta, R. S., Knight, J. F., Ediriwickrema, J., Lyon, J. G. and Worthy, L. D. 2006. Land-cover change detection using multi-temporal MODIS NDVI data. Remote Sens Environ. **105**:142-154.
[27]Akbarzadeh, M., Kafaki, S. B., Shahrokhi, S., Ajalli, J. and Khodabandeh, H. 2011. Determining land use/land cover changes in Arsbaran region, North West of Iran. J. Food Agric. Environ. **9**(2):618-622.
[28]Chander, G. and Markham, B. 2003. Revised Landsat-5 TM radiometric calibration procedures and postcalibration dynamic ranges. IEEE T. Geosci. Remote **41**:2674-2677.
[29]Chander, G., Markham, B. L. and Helder, D. L. 2009. Summary of current radiometric calibration coefficients for Landsat MSS, TM, ETM+ and EO-1 ALI sensors. Remote Sens. Environ. **113**(5):893-903.
[30]Masuda, K., Takashima, T. and Takayama, Y. 1988. Emissivity of pure and sea waters for the model sea surface in the infrared window region. Remote Sens. Environ. **24**:313-332.
[31]Gong, A. D., Jiang, Z. Y., Li, J., Chen, Y. H. and Hu, H. L. 2005. Urban land surface temperature retrieval based on Landsat TM remote sensing images in Beijing. Remote Sensing Information **3**:18-20.
[32]Van De Griend, A. A. and Owe, M. 1993. On the relationship between thermal emissivity and the normalized difference vegetation index for nature surfaces. Int. J. Remote Sensing **14**(6):1119-1131.
[33]Artis, D. A. and Carnahan, W. H. 1982. Survey of emissivity variability in thermography of urban areas. Remote Sens. Environ. **12**:313-329.
[34]Weng, Q. 2003. Fractal analysis of satellite-detected urban heat island effect. Photogramm. Eng. Rem. S. **69**(5):555-566.
[35]Liu, X. P., Zhang, W. J., Liu, Z. J., Qu, F. and Song, W. F. 2010. Impacts of land cover changes on soil chemical properties in Taihang Mountain, China. J. Food Agric. Environ. **8**(3&4): 985-990.